ANTIOXIDANTS & REDOX SIGNALING
Volume 12, Number 9, 2010
© Mary Ann Liebert, Inc.
DOI: 10.1089/ars.2009.2945

The Hydrogen Sulfide Donor NaHS Promotes Angiogenesis in a Rat Model of Hind Limb Ischemia

Ming-Jie Wang,[1] Wen-Jie Cai,[2] Na Li,[1] Ying-Jiong Ding,[1] Ying Chen,[1] and Yi-Chun Zhu[1]

Abstract

It is not known whether H_2S can promote angiogenesis with improvement of regional blood flow in ischemic organs. Sodium hydrosulfide (NaHS, a H_2S donor) was administered once a day for 4 w following femoral artery ligation. Collateral vessel growth, capillary density, regional tissue blood flow, the expression of endothelial growth factor (VEGF), VEGF receptor 2 (VEGFR2) and Akt were examined during or at the end of the treatment period. NaHS treatment significantly increased collateral vessel growth, capillary density, and regional tissue blood flow in ischemic hind limb muscles compared with the controls. These effects were associated with an increase in VEGF expression in the skeletal muscles and VEGFR2 phosphorylation in the neighboring vascular endothelial cells, suggesting a role of VEGF in mediating the NaHS effects in a cell–cell interaction pattern. Moreover, NaHS treatment also resulted in an increase in Akt phosphorylation in ischemic hind limb muscles. In conclusion, our observations with NaHS strongly suggest that H_2S is a proangiogenic factor in chronic ischemia. The proangiogenic effect of NaHS may be mediated by interaction between the upregulated VEGF in the skeletal muscle cells and the VEGFR2 as well as its downstream signaling element Akt in the vascular endothelial cells. *Antioxid. Redox Signal.* 12, 1065–1077.

Introduction

Hydrogen sulfide (H_2S) is endogenously generated from cysteine by enzymes such as cystathionine β-synthase (CBS), cystathionine γ-lyase (CSE), and 3-mercaptopyruvate sulfur transferase (MST) (9,15, 25, 28). CBS and CSE are predominantly expressed in certain tissues (11). CBS is highly expressed in the hippocampus and cerebellum in mammalian brains (16), while CSE is the predominant H_2S forming enzyme in the vasculature in both vascular smooth muscle cells and endothelial cells (38). The concentration of H_2S in the plasma ranges from 20 to 80 μmol/L (35). H_2S has been recognized to play a pivotal role in cardiovascular physiology and diseases (18, 29). Sodium hydrosulfide (NaHS, H_2S donor) and saturated H_2S solution are used as a source of exogenous H_2S in these studies. For example, NaHS and H_2S solution has been shown to dilate rat aortic tissues by opening the ATP-sensitive potassium channels (K_{ATP} channels) in vascular smooth muscle cells and cause a transient decrease in blood pressure in anesthetized rats (19, 41). NaHS exerts a negative inotropic effect by inhibiting the L-type calcium channels in cardiomyocytes (27). Exogenous administration of NaHS attenuates the development of hypertension and prevents left ventricular remodeling in spontaneously hypertensive rats (23, 37). NaHS also exhibits proinflammatory activity such as an increase in neutrophil infiltration in lung tissues with an increase in plasma TNF-α concentrations (17).

However, little is known about the proangiogenic role of H_2S. We provide the first piece of evidence regarding the proangiogenic effect of exogenously administered NaHS. In cultured vascular endothelial cells, NaHS promotes proliferation, migration, and tube-like structure formation of the cells by inducing phosphorylation of Akt (2). The proangiogenic effect of NaHS is also observed in a model of vascular endothelial cell infiltration into Matrigel that is embedded under the abdominal skin of mice (2), whereas the Matrigel only contains extracellular matrix without any type of cells of a specific organ such as the cardiomyocytes or the skeletal muscle cells. Thus, the data obtained in this model fell short in representing the process of angiogenesis in a specific organ. Moreover, a more clinically relevant question regarding whether an H_2S donor can promote angiogenesis in a specific ischemic organ remains to be investigated. In an ischemic organ, angiogenesis occurs in a hypoxic environment where certain cell types such as cardiomyocytes or skeletal muscle cells are present. To date, there is no information about the possible proangiogenic role of H_2S in any *in vivo* ischemic models.

[1]Department of Physiology and Pathophysiology, Fudan University Shanghai Medical College, Shanghai, China.
[2]Department of Basic Medicine, University of Shanghai for Science and Technology, Shanghai, China.

In ischemic organs, the process of angiogenesis is more complicated than what we have observed in cultured cells and the Matrigel model (2). Chronic ischemia itself may induce angiogenesis and thus consequently ameliorate the blood supply for the ischemic tissue (3). Moreover, the main cells types of the organ such as cardiomyocytes or skeletal muscle cells may interact with growing vascular endothelial cells by secreting certain proangiogenic factors such as VEGF, bFGF, angiopoietin-1, and transforming growth factor-beta (TGFβ) (5, 8, 36). Thus, whether the angiogenesis promoting factors like VEGF can be induced in any type of cells in H_2S-induced angiogenesis is also worthy of investigation. In this context, VEGF released upon NaHS stimulation may act on the VEGFR2 receptors in the vascular endothelial cells and thus promote the growth of the vasculature.

Therefore, the present study aimed to test the hypothesis that H_2S might promote angiogenesis in an *in vivo* ischemic model of hind limb ischemia in rats. The role of VEGF and the cell types expressing VEGF and its receptor were also investigated. Since phosphorylation of Akt has been shown to mediate the proangiogenic effects of H_2S donor in cultured vascular endothelial cells (2), the expression of both the total and phosphorylated forms of this signaling element were also examined.

Materials and Methods

Rat model of unilateral hind limb ischemia

Male Wistar rats (200–250 g, obtained from the Department of Experimental Animals, Chinese Academy of Sciences, Shanghai, China) were subjected to unilateral femoral artery ligation (4, 26) under anesthesia with intraperitoneal administration of chloral hydrate (300 mg/kg) after 3–4 days of acclimation. A vertical incision was made along the inner left hind limb. The left femoral artery was exposed, ligated with 5-0 silk ligatures, and a 5 mm long section of the artery was excised without damaging the vein and nerve. The right limb served as an internal control for each rat. All animal procedures conformed to the "Guide for the Care and Use of Laboratory Animals" published by the National Institutes of Health (NIH) of the United States and was approved by the Ethics Committee of Experimental Research, Fudan University Shanghai Medical College. Animals were randomly allocated to six groups: vehicle, NaHS (Sigma, St Louis, MO) intraperitoneal injection (10, 20, 50, 100, or 200 μmol·kg^{-1}·day^{-1}). H_2S was administered in the form of NaHS which has been well established as a reliable donor of H_2S (17).

Histological examinations

Rat hind limb gastrocnemius muscle was excised 1 h after administration of NaHS or 1 w after femoral artery ligation with or without treatment for examination of inflammatory cell infiltration, VEGF, VEGFR2, and Phospho-VEGFR2 expression (2 w) or capillary density determination (1, 2, and 4 w). Samples were fixed in buffering formalin, and embedded in low melting point paraffin. Five plugs in each group were used for histological examinations. Staining was performed with 5 μm-thick transverse sections.

Hematoxylin and eosin staining was used for examination of inflammatory cell infiltration. Capillaries were recognized with a goat polyclonal anti-rat CD34 antibody (AF4117, R&D Systems, MN) followed by staining with a horseradish peroxidase-conjugated secondary antibody and the diaminobenzidine substrate. For double staining, the secondary antibody was alkaline phosphatase conjugated and BCIP/NBT served as substrate. The proliferating cells in the tissues were detected with proliferating cell nuclear antigen (PCNA) staining using a mouse monoclonal anti-PCNA antibody (2586, Cell Signaling Technology, Danvers, MA). VEGF expression was determined with a monoclonal antibody (sc-7269, Santa Cruz Biotechnology, Santa Cruz, CA). VEGFR2 (2472, Cell Signaling Technology) and Phospho-VEGFR2 (Tyr996, 2474, Cell Signaling Technology) rabbit monoclonal antibody were used to detect total and phosphorylated VEGFR2. Capillaries or VEGFR2 positive cells were counted in 10 randomly chosen, nonoverlapping fields. Photographs of histological sections were taken using a Leica microscope (Leica, Wetzlar, Germany).

Recording of the hemodynamic parameters

Rats were anesthetized with chloral hydrate (300 mg/kg) on day 27 post femoral artery occlusion (one day before regional blood flow measurement or capillary density determination). A PE-50 catheter was inserted into the left carotid artery and was exteriorized at the nape of the neck. On the following day (day 28), the arterial catheter was connected to a pressure transducer. After an equilibrium period of 30 min, systolic blood pressure (SBP), diastolic blood pressure (DBP), mean arterial pressure (MAP), and heart rate (HR) were recorded in conscious, freely moving animals for 30 min.

Microangiography

Rats were anesthetized with chloral hydrate (300 mg/kg) on day 28 post femoral artery occlusion, and a medial laparotomy was performed. The infrarenal abdominal aorta was ligated proximally and cannulated distally with a PE-50 catheter to the abdominal aorta 1 cm proximal to the iliac bifurcation. The lower hind limbs were perfused with 2 ml of warm heparinized saline (10 U/mL), and animals were euthanized by an overdose of chloral hydrate. Postmortem microangiography was then performed as described before (7, 13) with some modifications. Nitroglycerine (200 μg, Sigma Aldrich) was delivered through the catheter into the distal abdominal aorta to induce maximal vasodilatation (31), followed by a perfusion of 2 ml saline. After a period of 1 min, 3 ml of 60% iodinated contrast medium (SunRise, Shanghai, China) was manually injected. Images were acquired with an X-ray mammography system (Faxitron, Lincolnshire, IL) from the level of the left common iliac artery to the distal end of the ischemic limb to image the morphological development of collateral vessels. The films showing the medial thigh area of the ischemic limbs were used to quantify the amount of collateral vessels. After completing the microangiography procedures, the catheters were removed and the wounds were closed.

Quantitative angiographic analysis of collateral vessel growth was performed by measuring the total length of the contrast-opacified vessels by an observer blinded to the treatment regimen. The area of interest was outlined with the site of ligature on the femoral artery, the knee, the edge of the femur, and the external limit of the leg. The angiographic score was calculated as the ratio of total vessel length in the

ischemic limb to that of the non-ischemic limb in each animal using the software Image (NIH, Bethesda, MD).

Regional blood flow measurement with microsphere assay

The regional blood flow in skeletal muscles in both hind limbs of the rats was measured by using fluorescent microspheres at the end of the 4 w NaHS treatment period (24) with some modifications. Briefly, the rats were anesthetized intraperitoneally with chloral hydrate (300 mg/kg) and a PE-50 catheter was inserted into the aortic arch *via* the carotid artery for microsphere injection. Both kidneys were ligated to increase the microsphere density in the hind limbs. Microspheres (0.4 ml, 4×10^5 microsphere beads, 15 μm diameter, Molecular Probes, Eugene, OR) were injected at a rate of 0.4 ml/min and were flushed with 0.5 ml of 0.9% saline at a rate of 0.3 ml/min. Injection time was precisely managed to 1 min in order to avoid streaming of spheres that may occur if bolus injection is performed. Then the animals were euthanized and the adductor and gastrocnemius muscles of both limbs were excised. Each muscle sample was weighed, cut into small pieces with sterile scissors, and digested in 3 ml/g tissue of 2 mol/L ethanolic KOH containing 0.5% Tween 80 at 60°C for 48 h with constant shaking. After complete digestion of the tissues, the microspheres were collected by centrifugation at 2000 *g* for 20 min and washing sequentially with 10 ml deionized water with and without 0.25% Tween 80. Finally, microspheres were dissolved in 3 ml of 2-ethoxyethylacetate and the intensity of fluorescence was determined by using a fluorescence spectrometer (TECAN, Männedorf, Switzerland) at 570/598 nm. The regional blood flow in the ischemic limb was standardized with tissue weight and represented as the ratio of fluorescence intensity in the ischemic hind limb to that of the contralateral nonischemic hind limb in each animal.

Measurement of plasma H_2S concentration

Plasma H_2S concentrations were measured using a spectrophotometric approach at baseline or at 30 min, 1 h, 3 h, or 6 h after intraperitoneal injection of 50 μmol $\cdot$ kg^{-1} NaHS as described elsewhere (2). Briefly, 0.1 ml plasma was added into a test tube containing 0.125 ml 1% zinc acetate and 0.15 ml distilled water. Then 0.067 ml 20 m*M* N,N-dimethylphenylenediamine dihydrochloride in 7.2 *M* HCl was added. This was followed by addition of 0.067 ml 30 m*M* $FeCl_3$ in 1.2 *M* HCl. After the proteins in plasma were removed by adding 0.125 ml 10% trichloroacetic acid, absorbance of the resulting solution was measured with a spectrometer (TECAN) at a wave length of 670 nm. The concentration of H_2S in the solution was calculated according to the calibration curve of the standard H_2S solution at concentrations from 6.25 to 100 μ*M*.

Measurement of plasma nitrate/nitrite

Plasma nitrate/nitrite (NOx) was determined with a spectrometer using the Greiss reagent, as described elsewhere (17). Briefly, 60 μl plasma were incubated (37°C, 30 min) with nitrate reductase (10 mU) in the presence of NADPH (100 μ*M*) to reduce nitrate to nitrite and then centrifuged (14,000 *g*, 25 min, 4°C). The resulting supernatant and sodium nitrite standard were added in duplicate to 96-well microtiter plates. Thereafter, Griess reagent was added into the above mixture in a ratio of 1:1 (v/v) and incubated for 10 min at room temperature, after which absorbance was determined at 540 nm with a spectrometer (TECAN). The concentration of NOx was calculated from a standard curve of $NaNO_2$ at concentrations from 0.125 to 75 μ*M*.

Western blot analysis

VEGF expression and phosphorylation of Akt in ischemic gastrocnemius muscles were measured using Western blot analysis. Muscle samples taken 2 w after femoral artery ligation were collected and homogenized in pre-cooled 1X SDS lysis buffer (62.5 mmol/L Tris-HCl, pH 6.8 at 25°C; 2% w/v SDS; 10% glycerol; 50 mmol/L DTT). Protein concentration was determined by the BCA protein assay kit (Pierce Chemical Co., Rockford, IL). Thirty microgram protein was separated on a 10% SDS-polyacrylamide gel for Akt or a 15% SDS-polyacrylamide gel for VEGF and then transferred to a PDVF membrane (BioRad, Hercules, CA). After blocking with TBST containing 5% milk for VEGF or 5% BSA for Akt at room temperature for 1 h, the membrane was incubated with antibodies against Akt (Cell Signaling Technology) or VEGF (SC-507, Santa Cruz Biotechnology) overnight at 4°C. Anti-actin (SC-1616-r, Santa Cruz Biotechnology) was blotted as protein loading control. After incubation in horseradish peroxidase-conjugated secondary antibodies for 1 h at room temperature, SuperSignal West Pico Chemiluminescent Substrate was used for detection of the blotting signals.

Statistical analysis

Results are expressed as mean $\pm$ SEM. Differences between groups were analyzed by one-way ANOVA followed by post hoc Tukey's test where applicable. Significance was established at the $p < 0.05$ level.

Results

Effects of NaHS on inflammatory cell infiltration in hind limb muscles

HE staining of muscle sections was examined for inflammatory cell infiltration in hind limb muscles at 1 h and 1 w after NaHS treatment (50 μmol $\cdot$ kg^{-1}). As shown in Fig. 1A, inflammatory cell infiltration was not found in sections of ischemic hind limb muscles or in that of nonischemic hind limb muscles.

Effects of chronic NaHS treatment on blood pressure in Wistar rats

Blood pressure and heart rate were measured in freely moving conscious rats before sacrifice on day 28 (NaHS was not administered on that day). As shown in Fig. 1B, NaHS treatment did not cause any significant changes in blood pressure or heart rate as compared with that of vehicle-treated rats, whereas a single intraperitoneal injection of NaHS (50 μmol $\cdot$ kg^{-1}) caused an increase in plasma H_2S levels during the period from 10 min to 1 h after injection (Fig. 1C).

NaHS promoted collateral vessel growth in ischemic hind limbs

Angiographic scores in the ischemic/nonischemic hind limbs were obtained from microangiography 4 w after surgery

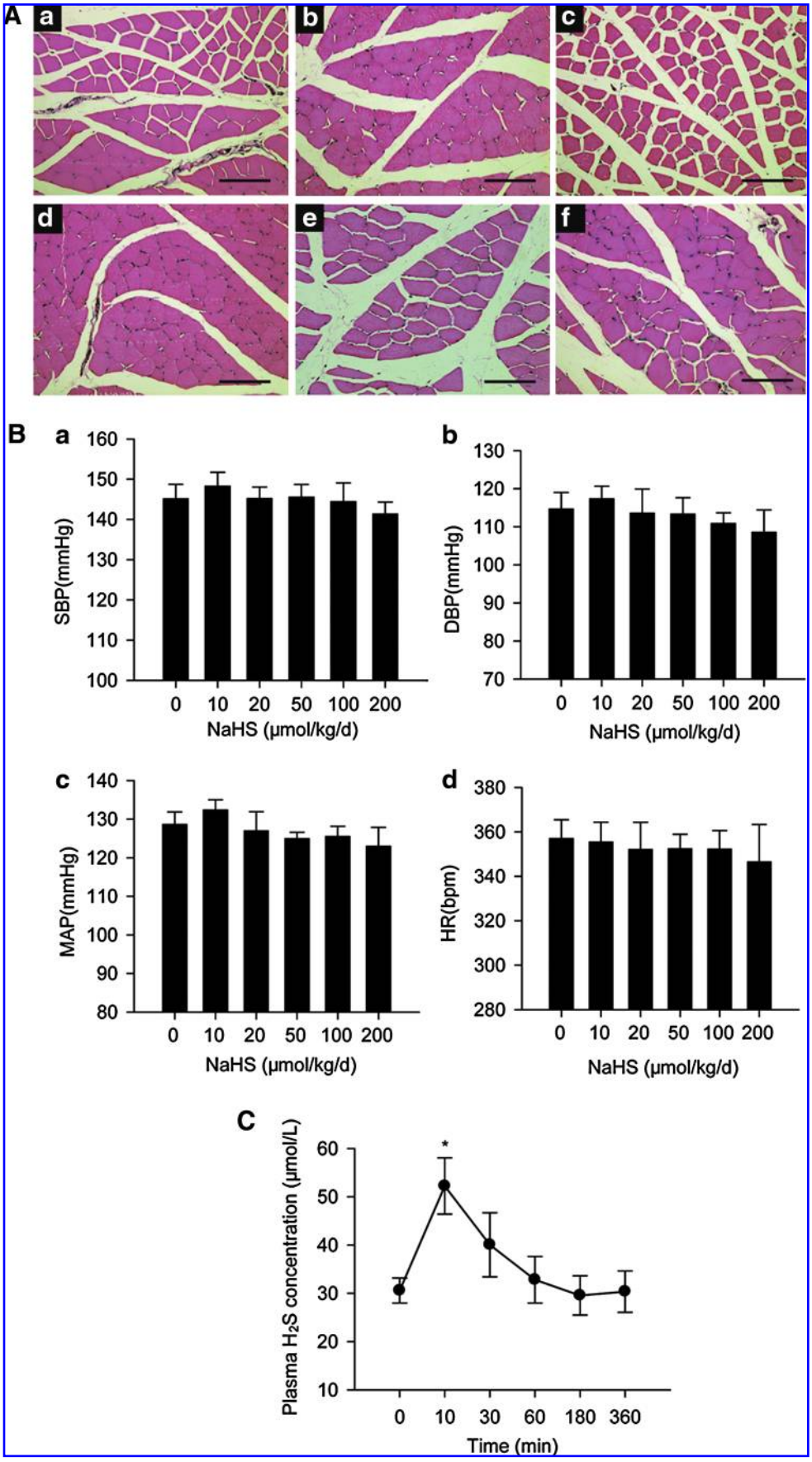
A
a
b
c
d
e
f
B
a
SBP(mmHg)
160
150
140
130
120
110
100
0 10 20 50 100 200
NaHS (μmol/kg/d)
b
DBP(mmHg)
130
120
110
100
90
80
70
0 10 20 50 100 200
NaHS (μmol/kg/d)
c
MAP(mmHg)
140
130
120
110
100
90
80
0 10 20 50 100 200
NaHS (μmol/kg/d)
d
HR(bpm)
380
360
340
320
300
280
0 10 20 50 100 200
NaHS (μmol/kg/d)
C
Plasma H2S concentration (μmol/L)
60
50
40
30
20
10
*
0 10 30 60 180 360
Time (min)

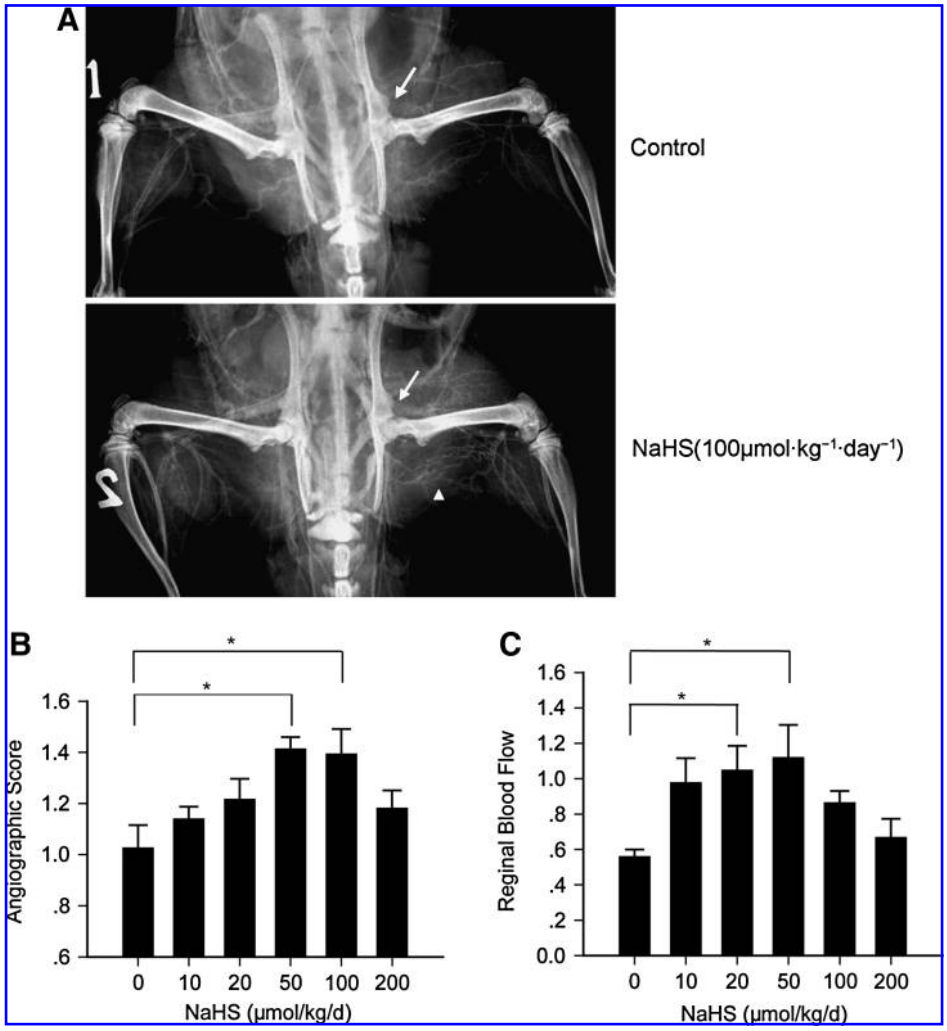

FIG. 2. NaHS treatment promoted collateral vessel formation and regional blood flow after femoral artery occlusion in the rat hind limb ischemia model. (**A**) Representative postmortem angiograms obtained 4 w after surgery. There was more collateral vessel formation in the ischemic left hind limb of the rats treated with NaHS at a dose of 100 μmol · kg^{-1} · day^{-1}. *Arrow* denotes the site of ligation at the femoral artery. *Arrow head* indicates the typical "corkscrew" appearance of collateral vessels. (**B**) Quantitative analysis of collateral vessel development was performed by measuring the total length of the contrast-opacified vessels. The angiographic score was significantly greater in the rats receiving NaHS (50 and 100 μmol · kg^{-1} · day^{-1}) than in the control animals (*$p < 0.05$ *vs.* vehicle by ANOVA). Data represent the mean ± SEM of three (10 and 20 μmol · kg^{-1} · day^{-1} NaHS) or five (the rest) experiments in each group. (**C**) Blood flow measured with microsphere assay. The regional blood flow in ischemic limb was standardized with tissue weight and represented as the ratio of fluorescence intensity in the ischemic hind limb to that of the contralateral nonischemic hind limb in each animal. NaHS treatment (20 and 50 μmol · kg^{-1} · day^{-1}) significantly improved regional blood flow in the ischemic limb (*$p < 0.05$ *vs.* vehicle by ANOVA). Data represent the mean ± SEM of nine (the control) or seven (the NaHS groups) experiments in each group.

with treatment of NaHS/vehicle. The nonischemic right hind limb served as an internal control. As shown in Fig. 2A, there were more angiographically visible collateral vessels with typical "corkscrew" appearance (arrow head) (33, 34) in the ischemic medial thigh area in the NaHS group as compared with that of the control group. The amount of collateral vessels in the ischemic medial thigh area was quantified with the angiographic scores (Fig. 2B). Angiographic scores at postoperative 4 w were significantly increased in the rats treated with NaHS at doses of 50 and 100 μmol · kg^{-1} · d^{-1} as compared with vehicle treatment (1.414 ± 0.0460 *vs.* 1.027 ± 0.0887 and 1.394 ± 0.0977 *vs.* 1.027 ± 0.0887, respectively; $p < 0.05$; Fig. 2B).

NaHS increased regional tissue blood flow in ischemic hind limbs

Regional tissue blood flow in the hind limbs was quantified with the fluorescent microspheres of 15 μm diameter which were injected into the thoracic aorta to indicate blood flow in the microvessels (11, 32). NaHS treatment caused a significant increase in regional blood flow in ischemic hind limbs

FIG. 1. NaHS treatment did not cause inflammation in hind limb muscles or alter the basic blood pressure in Wistar Rats. (**A**) Representative HE staining from normal rats (a), 1 h after 50 μmol · kg^{-1} NaHS administration (b, without surgery), 7 d after 50 μmol · kg^{-1} · day^{-1} NaHS administration (c from ischemic leg and d from nonischemic leg) and 7 d after vehicle administration (e from ischemic leg and f from nonischemic leg). Inflammatory cell infiltration in muscle sections was not found. *Bar* = 200 μm. (**B**) Quantitative analysis of systolic blood pressure (SBP, a), diastolic blood pressure (DBP, b), mean arterial pressure (MAP, c), and heart rate (HR, d) of conscious, freely moving rats just before sacrifice on day 28. There is no significant difference among NaHS groups and vehicle. Data represent the mean ± SEM of five experiments in each group. (**C**) Time course of plasma H_2S concentrations in rats after an intraperitoneal injection of NaHS (50 μmol · kg^{-1}). Data represent the mean ± SEM of four experiments in each group. Intraperitoneal injection of 50 μmol · kg^{-1} NaHS caused an increase in plasma H_2S levels from 10 min to 1 h after injection (*$p < 0.05$ *vs.* vehicle by ANOVA). (For interpretation of the references to color in this figure legend, the reader is referred to the web version of this article at www.liebertonline.com/ars).

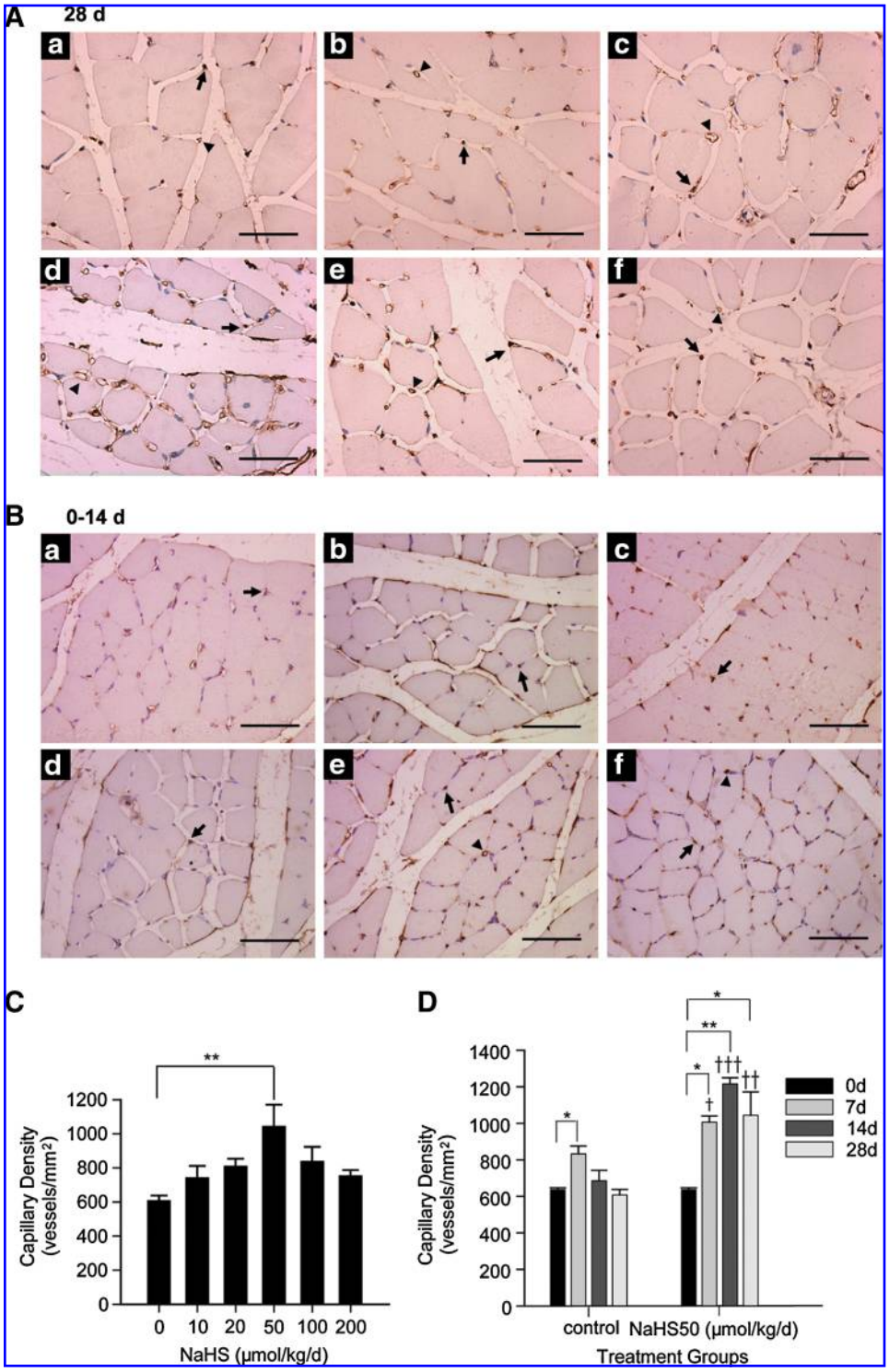

FIG. 3. NaHS treatment promoted the growth of microvessels after femoral artery occlusion. (**A**) Representative micrographs showing the vascular endothelial cells (*arrow*) and capillary vessels (*arrow head*) in the gastrocnemius muscles 4 w after surgery stained with anti-rat CD34 antibody. There were more capillaries developed in the ischemic hind limb muscles in the rats treated with NaHS (a for the vehicle, b, c, d, e, and f for 10, 20, 50, 100, and 200 μmol $\cdot$ kg^{-1} $\cdot$ day^{-1} NaHS groups, respectively). *Bar* = 100 μm. (**B**) Representative micrographs showing the time-course study of CD34 positive cells. a–c, control group (a, 0 d; b, 7 d; c, 14 d); d–f, 50 μmol $\cdot$ kg^{-1} $\cdot$ day^{-1} NaHS group (d, 0 d; e, 7 d; f, 14 d). *Bar* = 100 μm. (**C**) Quantitative analysis of the capillary density in ischemic gastrocnemius muscles 4 w after surgery. Results are expressed as number of capillary vessels/area of myofiber. Capillary density was significantly greater in the rats receiving NaHS (50 μmol $\cdot$ kg^{-1} $\cdot$ day^{-1}) than in the control animals (**$p < 0.01$ *vs.* vehicle by ANOVA). Data represent the mean ± SEM of five experiments in each group. (**D**) Quantitative analysis of the capillary density in time-course experiment. 50 μmol $\cdot$ kg^{-1} $\cdot$ day^{-1} NaHS treatment increased capillary density at day 7, peaked at day 14, and continued to be increased at the end of the experiment (day 28). *$p < 0.05$, **$p < 0.01$ *vs.* day 0; $^{\dagger}p < 0.05$, $^{\dagger\dagger}p < 0.01$, $^{\dagger\dagger\dagger}p < 0.001$ *vs.* control (at the same time point) by ANOVA. Data represent the mean ± SEM of four experiments in each group. (For interpretation of the references to color in this figure legend, the reader is referred to the web version of this article at www.liebertonline.com/ars).

at doses of 20 and 50 μmol $\cdot$ kg^{-1} $\cdot$ d^{-1} (1.048 $\pm$ 0.137 *vs.* 0.560 $\pm$ 0.0388 and 1.120 $\pm$ 0.184 *vs.* 0.560 $\pm$ 0.0388, respectively, $p < 0.05$; Fig. 2C).

NaHS caused an increase in capillary density

Since capillaries were not shown in the above-mentioned angiographic studies, vascular endothelial cells of the capillaries were visualized with immunohistochemical staining using specific endothelial cell markers. Capillary density was then assessed with the micrographs showing all the vascular endothelial cells in the hind limb sections. As shown in Fig. 3A and B, the vascular endothelial cells of capillary vessels in hind limb muscles were clearly stained with the anti-rat CD34 antibodies. NaHS treatment caused an increase in CD34-positive cells. Quantification of capillary density revealed a significant increase in capillary density in the group treated with NaHS at a dose of 50 μmol $\cdot$ kg^{-1} $\cdot$ d^{-1} comparing with the controls on day 28 (1,044.202 $\pm$ 127.425 vessels/mm^2 *vs.* 608.381 $\pm$ 29.268 vessels/mm^2, $p < 0.01$; Fig. 3C). Time-course experiment with the group treated with NaHS at a dose of 50 μmol $\cdot$ kg^{-1} $\cdot$ d^{-1} (Fig. 3D) revealed that NaHS treatment increased capillary density at day 7, peaked at day 14, and continued to be increased at the end of the experiment (day 28).

The micrographs (Fig. 3A and B) also showed that NaHS-induced increase in capillary density was not associated with any disorders in the morphology of the capillary network. There was no angioma formation observed in the NaHS-treated groups.

Immunostaining of PCNA and CD34 on two consecutive sections (Fig. 4) revealed that NaHS treatment (50 μmol $\cdot$ kg^{-1} $\cdot$ d^{-1}) promoted proliferation of the endothelial cells and the myocytes in the ischemic muscles.

NaHS treatment increased VEGF expression in ischemic hind limb muscles

VEGF protein expression in hind limb muscles was examined with immunohistochemistry and Western blot analysis 2 w after femoral artery ligation. As shown in Fig. 5A, VEGF signals (arrow) were found in the hind limb muscle sections and mainly localized in the skeletal muscle cells but not in the vascular endothelial cells. Double staining of VEGF and the vascular endothelial cells further clarified the cell types expressing VEGF in the groups treated with 50 μmol $\cdot$ kg^{-1} $\cdot$ d^{-1} NaHS administration and the vehicle (Fig. 5Ac and d).

To further quantify the amount of VEGF that was induced by NaHS treatment, Western blot analysis was performed with the hind limb muscle homogenates. VEGF protein expression was significantly increased following administration of NaHS at 20 and 50 μmol $\cdot$ kg^{-1} $\cdot$ d^{-1} as compared with the control (0.479 $\pm$ 0.0318 *vs.* 0.345 $\pm$ 0.0178 and 0.499 $\pm$ 0.0412 *vs.* 0.345 $\pm$ 0.0178, respectively; $p < 0.05$; Fig. 5B).

NaHS increased phosphorylation of VEGFR2 in vascular endothelial cells in ischemic hind limbs

The density of total VEGFR2 was not statistically altered by NaHS treatment (Fig. 6A and C).Phosphorylation of VEGFR-2 mediates most of the mitogenic and angiogenic effects of VEGF. Thus, the level of phospho-VEGFR2 (Tyr996) in ischemic hind limb muscles was examined with immunohistochemical staining. NaHS treatment caused an increase in phosphorylated VEGFR2 (Fig. 6B) which was localized in the vascular endothelial cells (Fig. 7). Quantification of the micrographs revealed a significant increase in the density of phosphorylated VEGFR2 at the Tyr996 site in group treated with NaHS at a dose of 50 μmol $\cdot$ kg^{-1} $\cdot$ d^{-1} as compared with the control (343.972 $\pm$ 41.738 positive cells/mm^2 *vs.* 163.623 $\pm$ 16.609 positive cells/mm^2, $p < 0.05$; Fig. 6D).

NaHS increased Akt phosphorylation in ischemic hind limb muscles

Akt phosphorylation was significantly increased following administration of 20–200 μmol $\cdot$ kg^{-1} $\cdot$ d^{-1} NaHS compared with control (Fig. 8A).

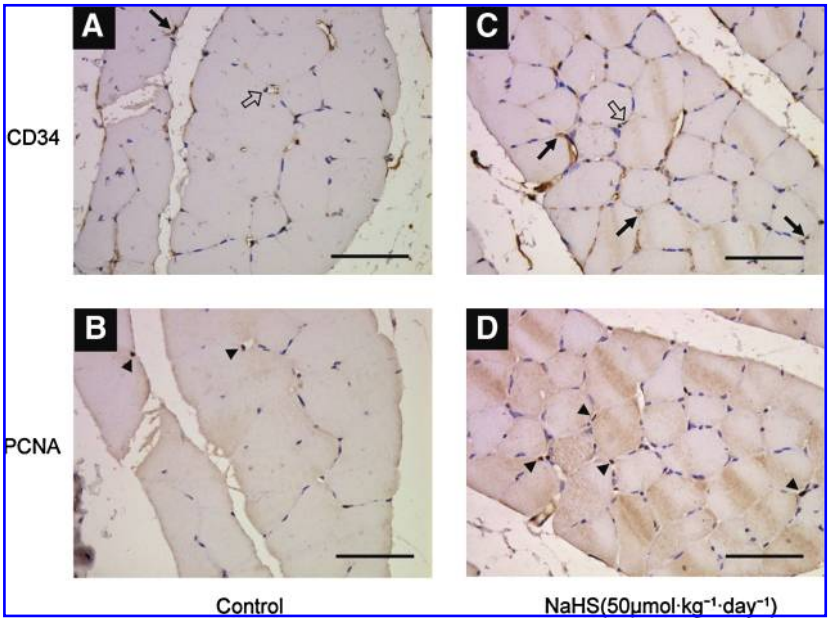

FIG. 4. NaHS treatment promoted cell proliferation in ischemic muscles. Immunohistochemistry was performed by using monoclonal antibodies against PCNA to show PCNA expression (*arrow head*) or polyclonal antibodies against CD34 to show the vascular endothelial cells (*arrow*) on two consecutive sections. PCNA expression (*arrow head*) was localized both in the nuclear of endothelial cells (*arrow*) and skeletal muscle cells (*hollow arrow*). NaHS treatment (50 μmol $\cdot$ kg^{-1} $\cdot$ d^{-1}) promoted PCNA expression in ischemic muscles. Bar = 100 μm

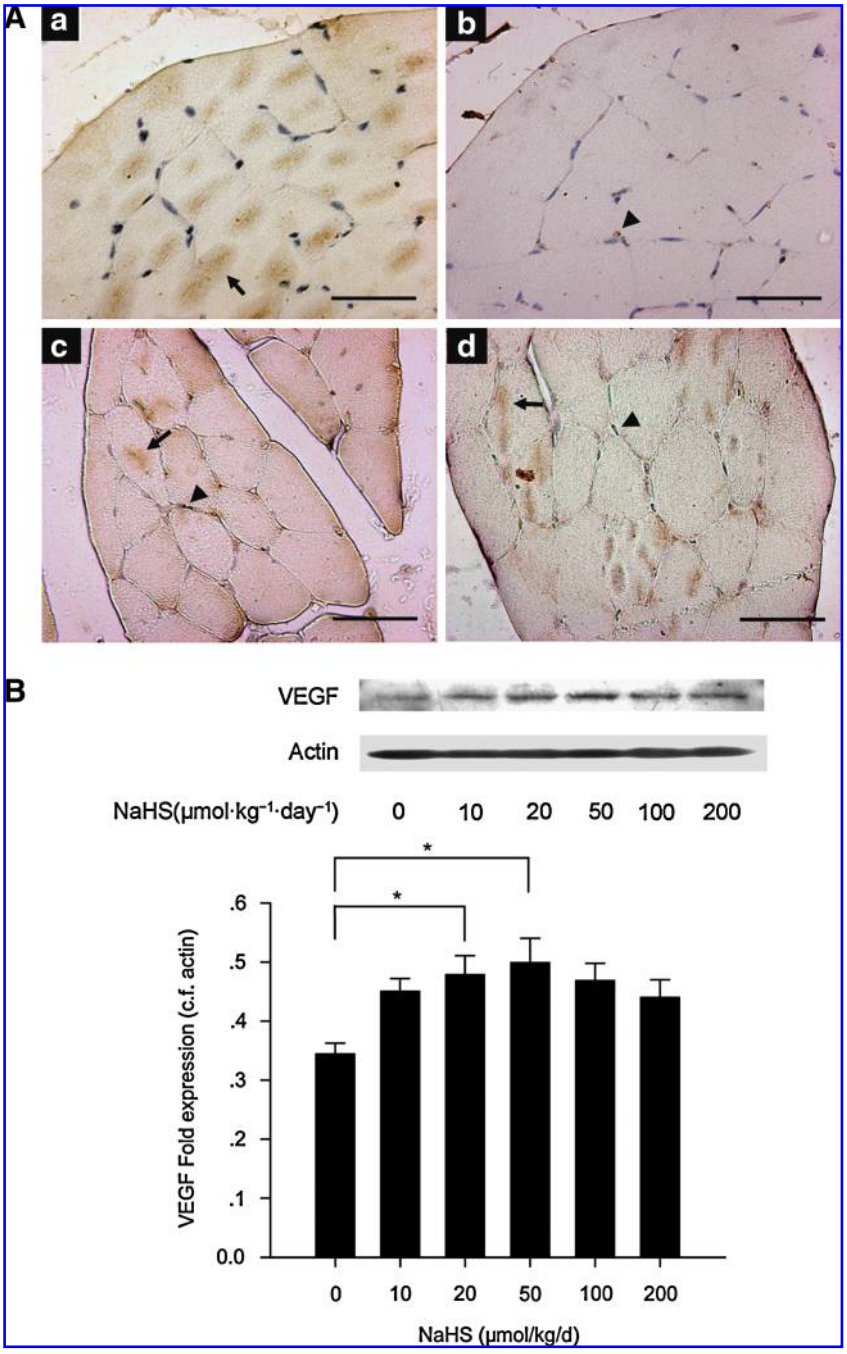

FIG. 5. NaHS increased VEGF expression in the ischemic hind limb muscles. (**A**) Tissue VEGF expression was mainly localized to the skeletal muscle cells. Immunohistochemistry was performed by using monoclonal antibodies against VEGF to show VEGF expression (*arrow*) or polyclonal antibodies against CD34 to show the vascular endothelial cells (*arrow head*). a and b, two consecutive sections showing that VEGF expression (*arrow*) was mainly localized in the skeletal muscle cells but not the vascular endothelial cells (*arrow head*). c and d, double staining of VEGF (*arrow*) and the vascular endothelial cells (*arrow head*) further clarified the skeletal muscle cells expressed VEGF in the groups treated with $50\,\mu mol \cdot kg^{-1} \cdot d^{-1}$ NaHS (d) and the vehicle (c). *Bar* = 100 μm. (**B**) Effects of treatment with various concentrations of NaHS ($10–200\,\mu mol \cdot kg^{-1} \cdot d^{-1}$) on VEGF expression. VEGF expression was significantly increased following administration of NaHS at 20 and $50\,\mu mol \cdot kg^{-1} \cdot d^{-1}$ for 2 w (*$p < 0.05$ *vs.* vehicle by ANOVA). Data represent the mean ± SEM of six independent experiments in each group. (For interpretation of the references to color in this figure legend, the reader is referred to the web version of this article at www.liebertonline.com/ars).

Effect of NaHS on plasma NOx concentrations

The plasma levels of nitric oxide (NO) metabolites in the group treated with NaHS ($50\,\mu mol \cdot kg^{-1} \cdot d^{-1}$) were not statistically different from that of the vehicle-treated group on day 7 (Fig. 8B).

Discussion

We have previously reported a proangiogenic effect of exogenously administered NaHS in cultured vascular endothelial cells and in Matrigel plugs embedded under the skin of mice (2). These findings were soon confirmed by Pyiochou *et al.* who found neovascularization induced by H_2S treatment in chicken chorioallantoic membranes (21). However, to date, there is no information regarding a purported proangiogenic role of H_2S in any *in vivo* ischemic models which is more clinically relevant. H_2S donors/precursors (such as NaHS, Na_2S) (40, 41) and the slow-releasing H_2S donor (GYY4137) (19) have been used as a source of exogenous H_2S in various laboratories worldwide. In the present study, NaHS was used as a H_2S donor. In aqueous solutions with a pH value of 7.4 at 37°C, 18.5% NaHS is transformed into H_2S and the rest remains as the HS^- ion (6), while the amount of Na^+ is negligible (12). Therefore, the protection observed in the present study is rather an effect of H_2S/HS^- than that of H_2S alone. However, the present methodology can not clarify whether the effects of NaHS are mediated by H_2S or HS^-.

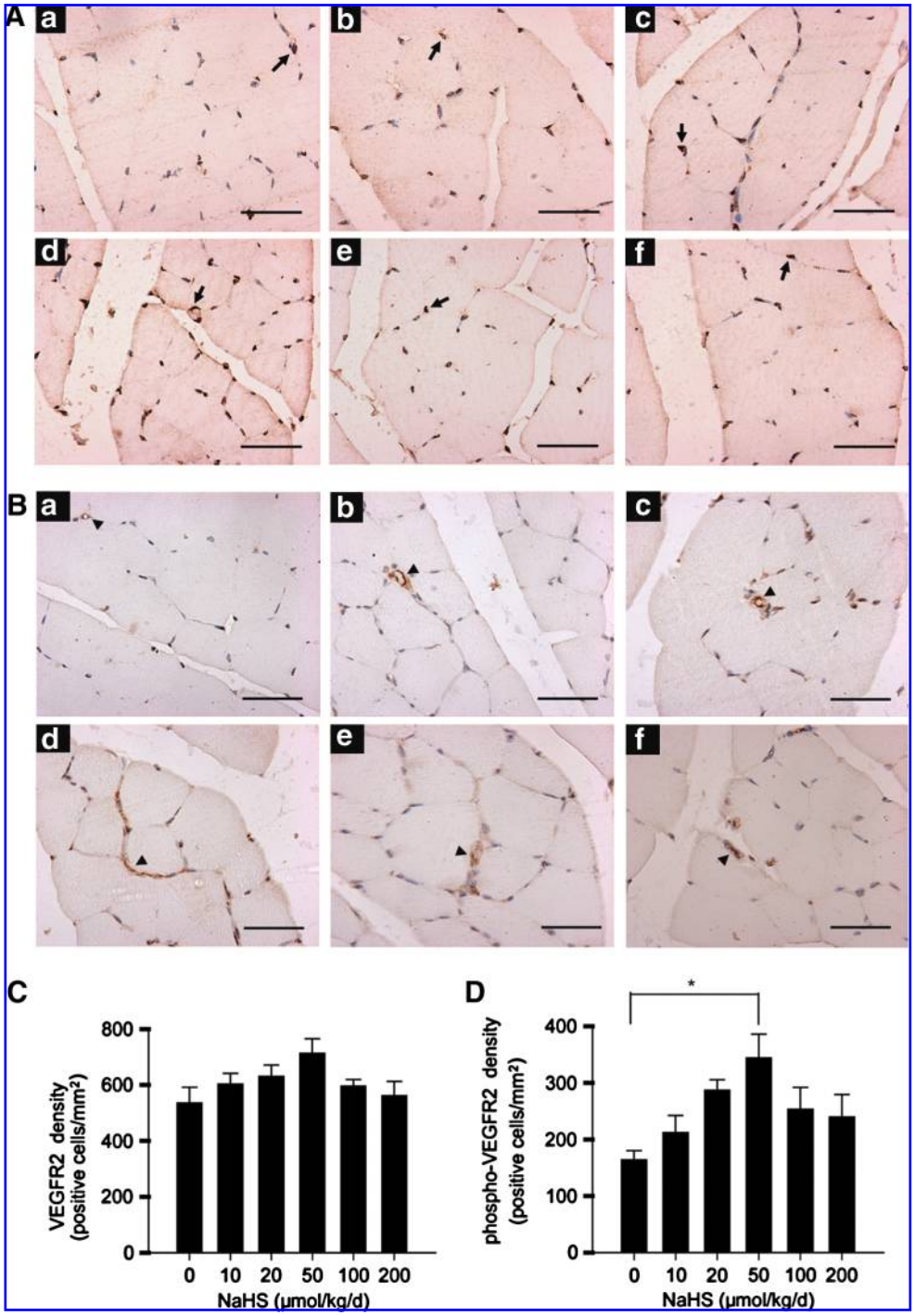

FIG. 6. Expression of total and phospho-VEGFR2 in endothelial cells in the ischemic hind limb muscles. (**A**) Representative micrographs of VEGFR2 (*arrow*) in the gastrocnemius muscles stained with anti- VEGFR2 antibodies (a for the vehicle, b, c, d, e, and f for 10, 20, 50, 100, and 200 μmol $\cdot$ kg^{-1} $\cdot$ day^{-1} NaHS groups, respectively). Total VEGFR2 expression was not altered by NaHS treatment. *Bar* = 100 μm. (**B**) Representative micrographs of phospho-VEGFR2 in the gastrocnemius muscles stained with the anti-phospho-VEGFR2 antibodies (a for the vehicle, b, c, d, e, and f for 10, 20, 50, 100, and 200 μmol $\cdot$ kg^{-1} $\cdot$ day^{-1} NaHS groups, respectively). Expression of phosphorylated VEGFR2 (*arrow head*) was significantly increased in the ischemic hind limb muscles of the rats treated with NaHS. *Bar* = 100 μm. (**C**) Quantitative analysis of VEGFR2 density in ischemic gastrocnemius muscles. VEGFR2 density was not statistically altered significantly by NaHS treatment. Data represent the mean $\pm$ SEM of four experiments in each group. (**D**) Quantitative analysis of phospho-VEGFR2 density. Phospho-VEGFR2 density was significantly greater in the rats receiving NaHS (50 μmol $\cdot$ kg^{-1} $\cdot$ day^{-1}) than in the control animals (*$p < 0.05$ *vs.* vehicle by ANOVA). Data represent the mean $\pm$ SEM of four experiments in each group.

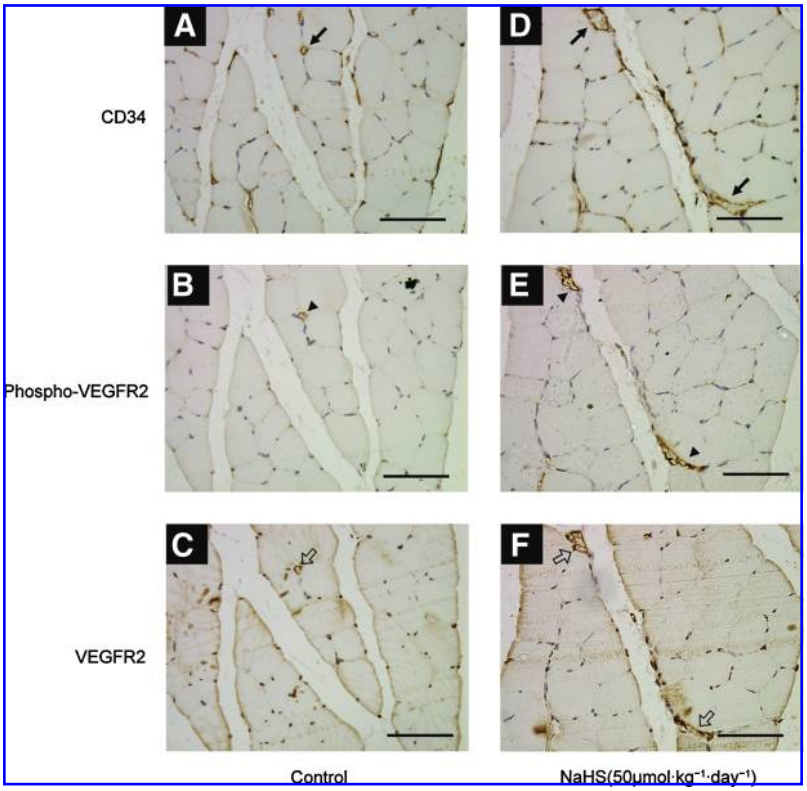

FIG. 7. Cellular localization of VEGFR2 and phospho-VEGFR2. (**A–C**) shows a set of three consecutive sections from vehicle group and (**D–F**) is another set of consecutive sections from $50\,\mu mol \cdot kg^{-1} \cdot d^{-1}$ NaHS group. Immunohistochemistry was done by using polyclonal antibodies against CD34 to show the vascular endothelial cells (*arrows* in A and D). Polyclonal antibodies against phospho-VEGFR2 or VEGFR2 were used to show phosphorylated VEGFR2 (*arrow heads* in B and E) or total VEGFR2 (*hollow arrows* in C and F). Comparison among the consecutive sections showed that the VEGFR2 and phospho-VEGFR2 signals were localized to endothelial cells. *Bar* = 100 μm. (For interpretation of the references to color in this figure legend, the reader is referred to the web version of this article at www.liebertonline.com/ars).

We found here that chronic treatment with NaHS for 4 w significantly promoted angiogenesis in ischemic hind limb muscles, suggesting that exogenous administration of NaHS may be further explored as a new approach for the treatment of chronic ischemic diseases. In our studies, NaHS treatment promoted the formation of collateral vessels in ischemic muscle tissues, suggesting a role of NaHS in promoting arteriogenesis which is a major event during collateral vessel growth (4). Moreover, NaHS treatment also promotes the growth of microvessels as indicated by an increase in capillary density and tissue blood flow of the microvessels. In the present study, NaHS-induced vessels formed vascular trees and capillary networks with improved tissue blood flow. That is in contrast with numerous experimental and clinical studies in which angioma was formed in tissues with injection of the vectors overexpressing VEGF which is a well-established pro-angiogenic factor (3, 22). It is obvious that the angioma induced by transfecting VEGF overexpressing vectors is not sufficient to establish functional network of the vessels to improve regional tissue blood flow. Thus, NaHS-induced angiogenesis in ischemic tissues has better morphology than that of the VEGF overexpression approaches. Worthy of notice is that NaHS at high dose ($200\,\mu mol \cdot kg^{-1} \cdot d^{-1}$) did not show any proangiogenic effect. One of the possible mechanisms is that H_2S/HS^- may bind to multiple cellular targets. At high doses, H_2S/HS^- may possibly act on certain additional cellular targets and evoke mechanism which may counter balance the proangiogenic pathways. These hypotheses remain to be further investigated.

Ling Li *et al.* reported that NaHS (14 μmol/kg ip) exhibits proinflammatory activities as evidenced by an increase in the infiltration of neutrophils in lung tissues associated with an increase in plasma TNF-α concentrations in mice (17). In the present study, histological examination showed there was no significant sign of neutrophil infiltration at time points of 1 h or 1 w after NaHS administration at a dose of $50\,\mu mol \cdot kg^{-1} \cdot d^{-1}$, suggesting that NaHS does not cause inflammation in skeletal muscles. This diversity may be ascribed to the difference in the models (rat *versus* mouse) used and the tissues (hind limb muscles *versus* lung) examined.

Exogenously administered H_2S has been shown to cause a transient decrease in blood pressure in anesthetized rats (19, 41). In the present study, NaHS ($50\,\mu mol \cdot kg^{-1} \cdot d^{-1}$) did not reduce blood pressure on day 28 when tissue blood flow and capillary density were measured. The data suggest that NaHS-induced increase in tissue blood flow and capillary density is not an effect secondary to an acute change in blood pressure. Indeed, we did not measure blood pressure at various time points during the 28-day treatment period. Therefore, whether NaHS caused any changes in blood pressure during the chronic treatment period remains unknown.

In the present study, we observed an increase in plasma H_2S levels at 10 min and lasted for 1 h after injection NaHS ($50\,\mu mol \cdot kg^{-1}$). Repeated chronic administration of NaHS in the present study (once a day for 27 days) may also contribute to the improvement observed. However, this hypothesis remains to be investigated by comparing the effects of single administration and repeated chronic treatment. Moreover, the effects of chronic NaHS treatment with a longer period also remain to be examined.

In the present study, NaHS treatment also caused significant increase in VEGF biosynthesis by Western blot analysis, and immunohistochemical staining further revealed that this increase in VEGF occurred in the skeletal muscles. VEGF has been shown to stimulate the growth of collateral vessels and capillaries in animal models of peripheral ischemia (31). In this context, VEGF synthesized in ischemic skeletal muscle cells may interact with the vascular endothelial cells in a

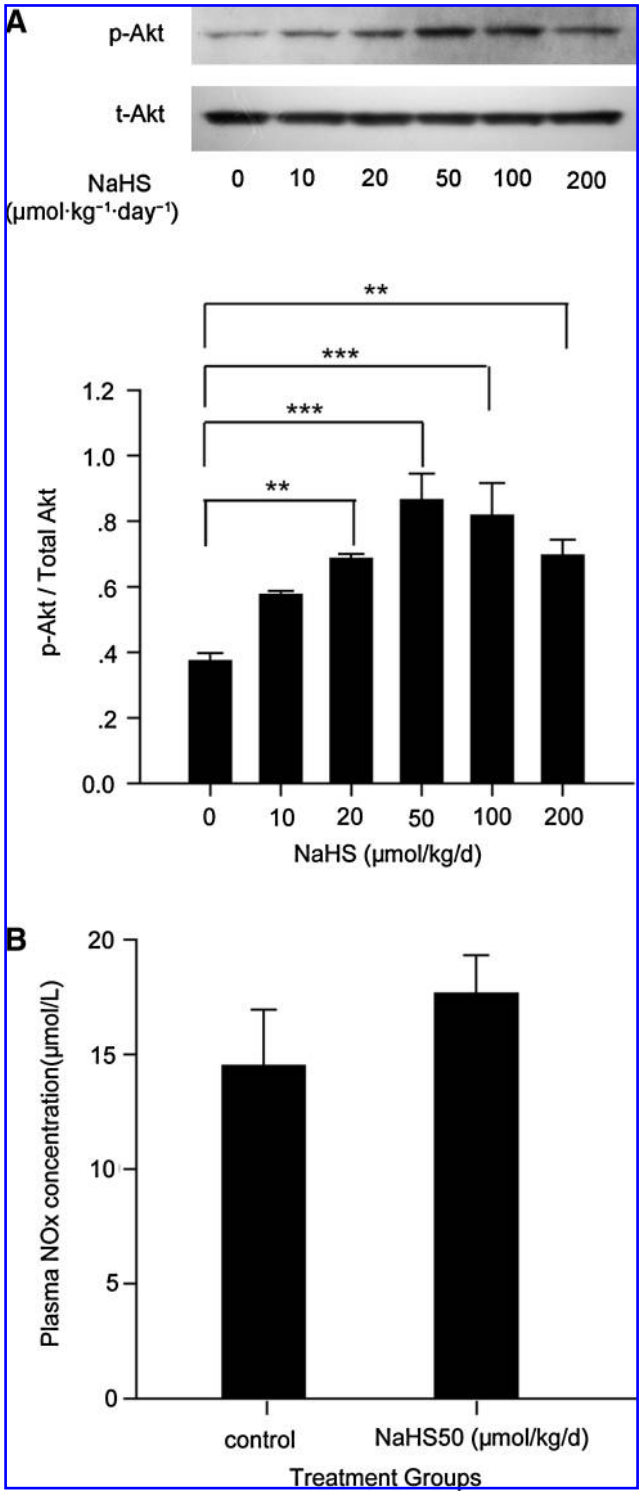

FIG. 8. NaHS increased Akt phosphorylation in ischemic hind limb muscles but did not alter plasma NOx concentration. (**A**) Akt phosphorylation was significantly increased following administration of NaHS at 20, 50, 100, and 200 μmol $\cdot$ kg^{-1} $\cdot$ d^{-1} for 2 w (**$p < 0.01$, ***$p < 0.001$ *vs.* vehicle by ANOVA). Data represent the mean $\pm$ SEM of five independent experiments in each group. (**B**) Plasma NO metabolites were not statistically different between NaHS (50 μmol $\cdot$ kg^{-1} $\cdot$ d^{-1}) treated group and vehicle-treated group. Data represent the mean $\pm$ SEM of four experiments in each group.

paracrine pattern. However, to date, there is no information regarding a promoting role of NaHS on VEGF biosynthesis. Our previous study shows that NaHS did not change VEGF expression in the vascular endothelial cells (2). The present data suggest a new mechanism of NaHS-induced angiogenesis (*i.e.*, VEGF biosynthesis may be stimulated by NaHS in the skeletal muscle cells and in turn to promote angiogenesis of the neighboring vascular endothelial cells in addition to the direct promoting effect of NaHS on the vascular endothelial cells) (2). The mechanisms regarding how NaHS can stimulate VEGF biosynthesis in the skeletal muscle cells remain to be further clarified.

VEGFR2 is the main receptor type to mediate the pro-angiogenic effect of VEGF (10), while VEGFR2 activation is insufficient in ischemic conditions (26). The present study showed that NaHS treatment resulted in significant increase in VEGFR2 phosphorylation in ischemic hind limb muscles compared with the vehicle treated animals, suggesting a role of VEGFR2 activation in NaHS-induced angiogenesis. Our data also revealed that phosphorylated VEGFR2 was mainly localized in vascular endothelial cells. In this context, NaHS-induced VEGFR2 activation in vascular endothelial cells may be ascribed to upregulated VEGF expression in the neighboring skeletal muscle cells.

In our previous studies, the pro-angiogenic effect of H_2S in cultured vascular endothelial cells is dependent on Akt phosphorylation. We found here that Akt phosphorylation was increased in ischemic hind limb muscles of the rats treated with NaHS. Thus, Akt may also be important in NaHS-induced angiogenesis in the *in vivo* ischemic models. However, the role of Akt in the *in vivo* conditions may be more complicated. Activation of Akt signaling has been reported to promote VEGF production in an autocrine manner in gastrocnemius muscles, induce myogenic differentiation and angiogenesis, and promote formation of collateral and capillary vessels (14, 30). Overexpression of Akt in skeletal muscles *in vivo* induces skeletal muscle hypertrophy, local VEGF production, and angiogenesis (30). Therefore, Akt may also mediate NaHS-induced increase in VEGF expression in ischemic skeletal muscle cells. However, the pathways between H_2S and Akt activation remain to be further investigated.

Gasotransmitter NO has also been recognized as a pro-angiogenic factor (42). On the other hand, H_2S was reported to interact with NO (1). In our previous studies, we did not find significant changes in NO metabolite levels in the culture medium of the endothelial cells. In the present study, NaHS treatment did not cause any significant changes in NO metabolite levels in the plasma 7 days after NaHS treatment, suggesting that NO was not involved in the proangiogenic effects of NaHS treatment. However, local NO levels in the ischemic muscles were not measured in the present study, nor were the activities of the NO synthases such as eNOS and iNOS. Further experiments are required to clarify the possible interaction of these two gasotransmitters in local ischemic tissues.

Chronic ischemia itself may induce angiogenesis that may in turn ameliorate blood supply of the ischemic tissue (3). However this self-protection mechanism is usually insufficient (20). As shown in the present study, capillary density is increased 1 w after surgery in both NaHS- and vehicle-treated groups, however, capillary density decreased to baseline levels at the time-points of 2 and 4 w in control group, whereas in the NaHS-treated groups, capillary density

continued to be increased till the end of the experiment period (day 28). An increase in capillary density may be mediated by VEGF that is released from the skeletal muscle cells upon NaHS stimulation and hence activate VEGFR2 in the neighboring vascular endothelial cells. Further experiments such as co-culture of the skeletal muscle and vascular endothelial cells are required to investigate this hypothesis of cell–cell interaction. Other possible mechanisms underlying NaHS-induced increase in capillary density include a direct proangiogenic action of NaHS on the local vascular endothelial cells and a recruitment of the endothelial progenitor cells released from the bone marrow. Our previous study showed that NaHS stimulated endothelial cell proliferation *in vitro* at concentrations of 10 and 20 μmol/l (2). The present PCNA staining for locally proliferating cells further confirmed that NaHS stimulated the proliferation of both vascular endothelial cells and myocytes *in vivo*. Whether the endothelial progenitor cells are involved in NaHS-induced angiogenesis *in vivo* is not known.

Therapeutic approaches promoting vascular growth may be beneficial for the patients who are not to undergo conventional revascularization operations (39). The present study provides the first piece of evidence that NaHS treatment is able to promote collateral vessel growth, improve regional blood flow, and increase capillary density in the *in vivo* ischemic model. These observations may be further explored to develop novel approaches to treat chronic ischemic diseases.

In conclusion, H_2S/HS^- are proangiogenic factors in the chronic ischemic model of unilateral femoral artery occlusion in rats. These effects may be mediated by an increase in VEGF expression in the skeletal muscle cells and hence stimulate the VEGFR2 in the vascular endothelial cells. Akt phosphorylation is associated with the proangiogenic effect of NaHS in chronic ischemic conditions.

Acknowledgments

We are grateful to Professor Hui-Ming Jin for his kindly advice on the experimental designs. This work was supported by grants from the Ministry of Science and Technology (2010CB912601; 2009ZX09303-006) of China, the National Natural Science Foundation of China (30825016), and the Natural Science Foundation of Shanghai (09XD1400400).

Author Disclosure Statement

No competing financial interests exist.

References

1. Ali MY, Ping CY, Mok YY, Ling L, Whiteman M, Bhatia M, and Moore PK. Regulation of vascular nitric oxide *in vitro* and *in vivo*; A new role for endogenous hydrogen sulphide? *Br J Pharmacol* 149: 625–634, 2006.
2. Cai WJ, Wang MJ, Moore PK, Jin HM, Yao T, and Zhu YC. The novel proangiogenic effect of hydrogen sulfide is dependent on Akt phosphorylation. *Cardiovasc Res* 76: 29–40, 2007.
3. Carmeliet P. Angiogenesis in health and disease. *Nat Med* 9: 653–660, 2003.
4. Chang DS, Su H, Tang GL, Brevetti LS, Sarkar R, Wang R, Kan YW, and Messina LM. Adeno-associated viral vector-mediated gene transfer of VEGF normalizes skeletal muscle oxygen tension and induces arteriogenesis in ischemic rat hind limb. *Mol Ther* 7: 44–51, 2003.
5. Dallabrida SM, Ismail N, Oberle JR, Himes BE, and Rupnick MA. Angiopoietin-1 promotes cardiac and skeletal myocyte survival through integrins. *Circ Res* 96: e8–24, 2005.
6. Dombkowski RA, Russell MJ, and Olson KR. Hydrogen sulfide as an endogenous regulator of vascular smooth muscle tone in trout. *Am J Physiol Regul Integr Comp Physiol* 286: R678–685, 2004.
7. Duan J, Murohara T, Ikeda H, Sasaki K–I, Shintani S, Akita T, Shimada T, and Imaizumi T. Hyperhomocysteinemia impairs angiogenesis in response to hind limb ischemia. *Arterioscler Thromb Vasc Biol* 20: 2579–2585, 2000.
8. Engelmann GL. Coordinate gene expression during neonatal rat heart development. A possible role for the myocyte in extracellular matrix biogenesis and capillary angiogenesis. *Cardiovasc Res* 27: 1598–1605, 1993.
9. Erickson PF, Maxwell IH, Su LJ, Baumann M, and Glode LM. Sequence of cDNA for rat cystathionine gamma-lyase and comparison of deduced amino acid sequence with related *Escherichia coli* enzymes. *Biochem J* 269: 335–340, 1990.
10. Ferrara N, Gerber HP, and LeCouter J. The biology of VEGF and its receptors. *Nat Med* 9: 669–676, 2003.
11. Hoefer IE. Something is rotten in the state of angiogenesis—H2S as gaseous stimulator of angiogenesis. *Cardiovasc Res* 76: 1–2, 2007.
12. Hosoki R, Matsuki N, and Kimura H. The possible role of hydrogen sulfide as an endogenous smooth muscle relaxant in synergy with nitric oxide. *Biochem Biophys Res Commun* 237: 527–531, 1997.
13. Jacobi J, Tam BYY, Wu G, Hoffman J, Cooke JP, and Kuo CJ. Adenoviral gene transfer with soluble vascular endothelial growth factor receptors impairs angiogenesis and perfusion in a murine model of hind limb ischemia. *Circulation* 110: 2424–2429, 2004.
14. Jiang BH, Aoki M, Zheng JZ, Li J, and Vogt PK. Myogenic signaling of phosphatidylinositol 3-kinase requires the serine-threonine kinase Akt/protein kinase B. *Proc Natl Acad Sci USA* 96: 2077–2081, 1999.
15. Kamoun P. Endogenous production of hydrogen sulfide in mammals. *Amino Acids* 26: 243–254, 2004.
16. Kery V, Bukovska G, and Kraus JP. Transsulfuration depends on heme in addition to pyridoxal 5′-phosphate. Cystathionine beta-synthase is a heme protein. *J Biol Chem* 269: 25283–25288, 1994.
17. Li L, Bhatia M, Zhu YZ, Zhu YC, Ramnath RD, Wang ZJ, Anuar FBM, Whiteman M, Salto–Tellez M, and Moore PK. Hydrogen sulfide is a novel mediator of lipopolysaccharide-induced inflammation in the mouse. *FASEB J* 19: 1196–1198, 2005.
18. Li L, Hsu A, and Moore PK. Actions and interactions of nitric oxide, carbon monoxide and hydrogen sulphide in the cardiovascular system and in inflammation - a tale of three gases! *Pharmacol Ther* 123: 386–400, 2009.
19. Li L, Whiteman M, Guan YY, Neo KL, Cheng Y, Lee SW, Zhao Y, Baskar R, Tan C-H, and Moore PK. Characterization of a novel, water-soluble hydrogen sulfide-releasing molecule (GYY4137): New insights into the biology of hydrogen sulfide. *Circulation* 117: 2351–2360, 2008.
20. Nessa A, Latif SA, Siddiqui NI, Hussain MA, Bhuiyan MR, Hossain MA, Akther A, and Rahman M. Angiogenesis: A novel therapeutic approach for ischemic heart disease. *Mymensingh Med J* 18: 264–272, 2009.
21. Pyiochou A, Papapetropoulos A, Olah G, Wintner E, Jeschke M, Branski L, Herndon D, Traber D, and Szabo C. The hydrogen sulfide donor IK-1001 stimulates neovascularization and improves wound healing. *FASEB J* 22: 912.42, 2008.

22. Schwarz ER, Speakman MT, Patterson M, Hale SS, Isner JM, Kedes LH, and Kloner RA. Evaluation of the effects of intramyocardial injection of DNA expressing vascular endothelial growth factor (VEGF) in a myocardial infarction model in the rat—Angiogenesis and angioma formation. *J Am Coll Cardiol* 35: 1323–1330, 2000.
23. Shi Y–X, Chen Y, Zhu Y–Z, Huang G–Y, Moore PK, Huang S–H, Yao T, and Zhu Y–C. Chronic sodium hydrosulfide treatment decreases medial thickening of intramyocardial coronary arterioles, interstitial fibrosis, and ROS production in spontaneously hypertensive rats. *Am J Physiol Heart Circ Physiol* 293: H2093–2100, 2007.
24. Smith RS, Jr., Lin K–F, Agata J, Chao L, and Chao J. Human endothelial nitric oxide synthase gene delivery promotes angiogenesis in a rat model of hind limb ischemia. *Arterioscler Thromb Vasc Biol* 22: 1279–1285, 2002.
25. Stipanuk MH and Beck PW. Characterization of the enzymic capacity for cysteine desulphhydration in liver and kidney of the rat. *Biochem J* 206: 267–277, 1982.
26. Sugano M, Tsuchida K, and Makino N. Intramuscular gene transfer of soluble tumor necrosis factor-{alpha} receptor 1 activates vascular endothelial growth factor receptor and accelerates angiogenesis in a rat model of hind limb ischemia. *Circulation* 109: 797–802, 2004.
27. Sun Y–G, Cao Y–X, Wang W–W, Ma S–F, Yao T, and Zhu Y–C. Hydrogen sulphide is an inhibitor of L-type calcium channels and mechanical contraction in rat cardiomyocytes. *Cardiovasc Res*79: 632–641, 2008.
28. Swaroop M, Bradley K, Ohura T, Tahara T, Roper MD, Rosenberg LE, and Kraus JP. Rat cystathionine beta-synthase: Gene organization and alternative splicing. *J Biol Chem* 267: 11455–11461, 1992.
29. Szabo C. Hydrogen sulphide and its therapeutic potential. *Nat Rev Drug Discov* 6: 917–935, 2007.
30. Takahashi H and Shibuya M. The vascular endothelial growth factor (VEGF)/VEGF receptor system and its role under physiological and pathological conditions. *Clin. Sci.* 109: 227–241, 2005.
31. Takeshita S, Zheng LP, Brogi E, Kearney M, Pu LQ, Bunting S, Ferrara N, Symes JF, and Isner JM. Therapeutic angiogenesis. A single intraarterial bolus of vascular endothelial growth factor augments revascularization in a rabbit ischemic hind limb model. *J Clin Invest* 93: 662–670, 1994.
32. Tojo T, Ushio–Fukai M, Yamaoka–Tojo M, Ikeda S, Patrushev N, and Alexander RW. Role of gp91phox (Nox2)-containing NAD(P)H oxidase in angiogenesis in response to hind limb ischemia. *Circulation* 111: 2347–2355, 2005.
33. Tritsaris K, Myren M, Ditlev SB, Hubschmann MV, van der Blom I, Hansen AJ, Olsen UB, Cao R, Zhang J, Jia T, Wahlberg E, Dissing S, and Cao Y. IL-20 is an arteriogenic cytokine that remodels collateral networks and improves functions of ischemic hind limbs. *Proc Natl Acad Sci USA* 104: 15364–15369, 2007.
34. Westerweel PE, Rookmaaker MB, van Zonneveld AJ, Bleys RL, Rabelink TJ, and Verhaar MC. A study of neovascularization in the rat ischemic hind limb using Araldite casting and Spalteholtz tissue clearing. *Cardiovasc Pathol* 14: 294–297, 2005.
35. Whiteman M and Moore PK. Hydrogen sulfide and the vasculature: A novel vasculoprotective entity and regulator of nitric oxide bioavailability? *J Cell Mol Med* 13: 488–507, 2009.
36. Wu G, Mannam AP, Wu J, Kirbis S, Shie J–L, Chen C, Laham RJ, Sellke FW, and Li J. Hypoxia induces myocyte-dependent COX-2 regulation in endothelial cells: Role of VEGF. *Am J Physiol Heart Circ Physiol* 285: H2420–2429, 2003.
37. Yan H, Du J, and Tang C. The possible role of hydrogen sulfide on the pathogenesis of spontaneous hypertension in rats. *Biochem Biophys Res Commun* 313: 22–27, 2004.
38. Yang G, Wu L, Jiang B, Yang W, Qi J, Cao K, Meng Q, Mustafa AK, Mu W, Zhang S, Snyder SH, and Wang R. H2S as a physiologic vasorelaxant: Hypertension in mice with deletion of cystathionine {gamma}-lyase. *Science* 322: 587–590, 2008.
39. Yla–Herttuala S and Alitalo K. Gene transfer as a tool to induce therapeutic vascular growth. *Nat Med* 9: 694–701, 2003.
40. Zanardo RCO, Brancaleone V, Distrutti E, Fiorucci S, Cirino G, and Wallace JL. Hydrogen sulfide is an endogenous modulator of leukocyte-mediated inflammation. *FASEB J.* 20: 2118–2120, 2006.
41. Zhao W, Zhang J, Lu Y, and Wang R. The vasorelaxant effect of H(2)S as a novel endogenous gaseous K(ATP) channel opener. *EMBO J* 20: 6008–6016, 2001.
42. Ziche M, Morbidelli L, Masini E, Amerini S, Granger HJ, Maggi CA, Geppetti P, and Ledda F. Nitric oxide mediates angiogenesis *in vivo* and endothelial cell growth and migration *in vitro* promoted by substance P. *J Clin Invest* 94: 2036–2044, 1994.

Address correspondence to:
Professor Yi-Chun Zhu
Department of Physiology and Pathophysiology
Fudan University Shanghai Medical College
138 Yi Xue Yuan Road
Shanghai 200032
China

E-mail: yczhu@shmu.edu.cn

Date of first submission to ARS Central, October 10, 2009; date of acceptance, October 19, 2009.

Abbreviations Used

ANOVA = analysis of variance
BCA = bicinchoninic acid
BSA = bovine serum albumin
CBS = cystathionine β-synthase
CSE = cystathionine γ-lyase
DBP = diastolic blood pressure
DTT = dithiothreitol
ECs = endothelial cells
HR = heart rate
H_2S = hydrogen sulfide
K_{ATP} channels = ATP-sensitive potassium channels
MAP = mean arterial pressure
MST = 3-mercaptopyruvate sulfur transferase
NaHS = sodium hydrosulfide
NO = nitric oxide
PCNA = proliferating cell nuclear antigen
PVDF = polyvinylidene fluoride
SBP = systolic blood pressure
SDS = sodium dodecylsulfate
TBST = tris-buffered saline tween-20
VEGF = vascular endothelial growth factor
VEGFR2 = vascular endothelial growth factor receptor 2

This article has been cited by:

1. Stefania Merighi, Stefania Gessi, Katia Varani, Debora Fazzi, Pier Andrea Borea. 2012. Hydrogen sulfide modulates the release of nitric oxide and VEGF in human keratinocytes. *Pharmacological Research* **66**:5, 428-436. [CrossRef]
2. Slava Epelman, W.H. Wilson Tang. 2012. H2S—The Newest Gaseous Messenger on the Block. *Journal of Cardiac Failure* **18**:8, 597-599. [CrossRef]
3. Neil Dufton, Jane Natividad, Elena F. Verdu, John L. Wallace. 2012. Hydrogen sulfide and resolution of acute inflammation: A comparative study utilizing a novel fluorescent probe. *Scientific Reports* **2**. . [CrossRef]
4. Luca Munaron, Daniele Avanzato, Francesco Moccia, Daniele Mancardi. 2012. Hydrogen sulfide as a regulator of calcium channels. *Cell Calcium* . [CrossRef]
5. Emanuela Pupo, Alessandra Fiorio Pla, Daniele Avanzato, Francesco Moccia, José-Everardo Avelino Cruz, Franco Tanzi, Annalisa Merlino, Daniele Mancardi, Luca Munaron. 2011. Hydrogen sulfide promotes calcium signals and migration in tumor-derived endothelial cells. *Free Radical Biology and Medicine* . [CrossRef]
6. Ling Li, Peter Rose, Philip K. Moore. 2011. Hydrogen Sulfide and Cell Signaling. *Annual Review of Pharmacology and Toxicology* **51**:1, 169-187. [CrossRef]
7. Guangdong Yang. 2011. Hydrogen sulfide in cell survival: a double-edged sword. *Expert Review of Clinical Pharmacology* **4**:1, 33-47. [CrossRef]
8. Yi-Hong Liu, Ming Lu, Jin-Song Bian. 2011. Hydrogen sulfide and renal ischemia. *Expert Review of Clinical Pharmacology* **4**:1, 49-61. [CrossRef]
9. Csaba Szabó, Andreas Papapetropoulos. 2010. Hydrogen sulfide and angiogenesis: mechanisms and applications. *British Journal of Pharmacology* no-no. [CrossRef]
10. Benjamin L. Predmore, David J. Lefer. 2010. Development of Hydrogen Sulfide-Based Therapeutics for Cardiovascular Disease. *Journal of Cardiovascular Translational Research* **3**:5, 487-498. [CrossRef]
11. Ming-Jie Wang, Wen-Jie Cai, Yi-Chun Zhu. 2010. Mechanisms of angiogenesis: Role of hydrogen sulphide. *Clinical and Experimental Pharmacology and Physiology* **37**:7, 764-771. [CrossRef]
12. Wen#Jie Cai, Ming#Jie Wang, Li#Hua Ju, Cheng Wang, Yi#Chun Zhu. 2010. Hydrogen sulfide induces human colon cancer cell proliferation: role of Akt, ERK and p21. *Cell Biology International* **34**:6, 565-572. [CrossRef]
13. Rui Wang . 2010. Hydrogen Sulfide: The Third Gasotransmitter in Biology and Medicine. *Antioxidants & Redox Signaling* **12**:9, 1061-1064. [Abstract] [Full Text HTML] [Full Text PDF] [Full Text PDF with Links]